# Recurrence Plots for Diesel Engine Variability Tests

Rafał Longwic[a], Grzegorz Litak[b], and Asok K. Sen[c]

[a] Department of Vehicles, Technical University of Lublin, Nadbystrzycka 36, PL-20-618 Lublin, Poland
[b] Department of Applied Mechanics, Technical University of Lublin, Nadbystrzycka 36, PL-20-618 Lublin, Poland
[c] Department of Mathematical Sciences, Indiana University, 402 N. Blackford Street, Indianapolis, IN 46202-3216, USA

Reprint requests to G. L.; E-mail: g.litak@pollub.pl

Z. Naturforsch. **64a,** 96 – 102 (2009); received May 5, 2008 / revised June 24, 2008

Cycle-to-cycle variations of maximum pressure in a diesel engine are studied by using the methods of recurrence plots and recurrence quantification analysis. The pressure variations are found to exhibit strong periodicities in low frequency bands and intermittent oscillations at higher frequencies. The results are confirmed by wavelet analysis.

*Key words:* Combustion; Pressure Oscillations; Recurrence Plots; Recurrence Quantification Analysis.

## 1. Introduction

In a spark ignition engine, cycle-to-cycle variations in the process variables pressure and heat release have been identified as harmful features which limit the overall power output of the engine [1 – 7]. There are several factors that contribute to pressure and heat release variations. They include the compositions of fresh fuel-air mixture and burned gases, and engine aerodynamics [8 – 12]. These factors lead to nonlinear dynamics in the combustion process and may result in chaotic oscillations of the process variables [4 – 6, 13 – 17]. Recently, nonlinear phenomena have also been observed in diesel [18, 19], LPG-fueled [20] and natural gas [21] engines.

The nonlinear dynamics in a combustion process can be detected from the statistical properties of the measured signals. In a spark ignition engine, time irreversibility of the heat release fluctuations has been demonstrated by several authors [10, 14, 22]. In a natural gas engine, Li and Yao [21] observed a transition from stochastic to nonlinear deterministic behaviour in pressure variations by changing the equivalence ratio from near-stoichiometric to very lean conditions. Wendeker et al. [12], Litak et al. [23], and Sen et al. [24] have proposed an intermittent mechanism leading to chaotic pressure oscillations in a spark ignition engine. In addition, Sen *et al.* [19] have observed nonlinear oscillations in pressure in a diesel engine. In the present paper, we continue our research on the analysis of pressure fluctuations in a diesel engine and present further results on their dynamical behaviour using the methods of recurrence plots (RPs) and recurrence quantification analysis (RQA); we confirm these results by the wavelet analysis. The main advantage of using RPs and RQA is that these approaches do not need very long time series. Apart from the steady state it is also possible to identify a transient behaviour. Particularly this property could be used in a more efficient real time engine control.

Our presentation is organized as follows. In Section 2 we describe the experimental setup and present the pressure time series. The time series are analyzed in Section 3 using the methods of RPs and RQA. We also perform a wavelet analysis of the time series and confirm some of the results obtained by RPs and RQA. Finally, in Section 4, a few concluding remarks are given.

## 2. Experimental Setup and Cyclic Peak Pressure Variations

Figure 1a shows a schematic diagram of the experimental stand. The diesel engine is fueled by standard diesel fuel and the in-cylinder pressure is measured under steady-state conditions, using a piezoelectric pressure sensor (8). From the sensor the signal is transferred through connecting wires to a charge am-

 

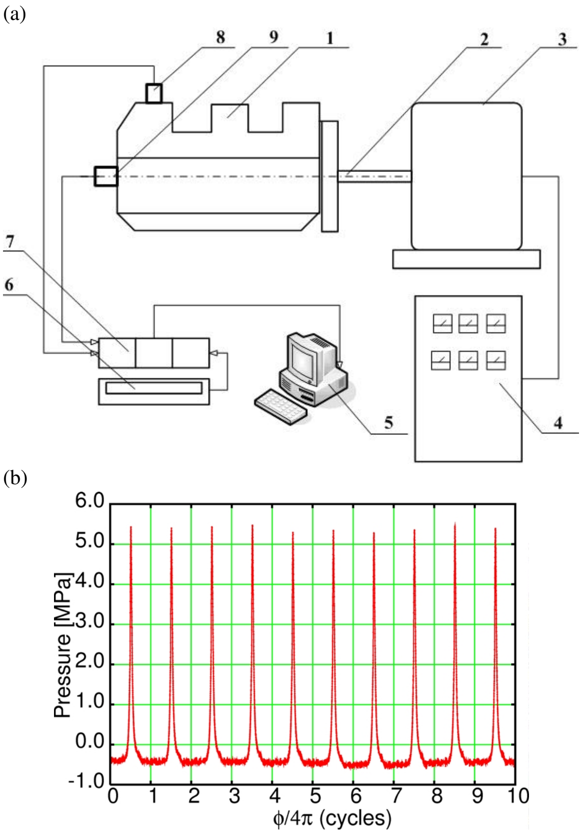


Fig. 1. (a) Experimental stand: 1, engine; 2, crankshaft; 3, brake; 4, brake control; 5, computer with data acquisition card; 6, signal generator; 7, amplifier; 8, piezoelectric pressure sensor. (b) The first 10 cycles of measured internal pressure versus crankshaft rotation angle $\phi$. Here $\Omega = 1200$ rpm and there are 1024 measurement points per cycle.

plifier (7), and then decoded by a computer with a data acquisition card (5).

The loading of the engine is controlled by an eddy-current brake coupled to the crankshaft. Pressure data are collected over 978 cycles for six different rotational speeds of the crankshaft: $\Omega = 1000$, 1200, 1400, 1600, 1800 and 2000 rpm under full loading. Measurements are made with a sampling frequency of 1024 times per combustion cycle.

An example of the measured pressure time series for $\Omega = 1200$ rpm is shown in Figure 1b. In order to study the cycle-to-cycle variability, it is convenient to use the peak values of the pressure [25, 26]. Accordingly, we have identified the peak pressure in each cycle from the time series shown in Fig. 1b, forming a peak-pressure time series; this is depicted in Fig. 2 for $\Omega = 1200$ rpm. This figure also shows the peak pressure time series

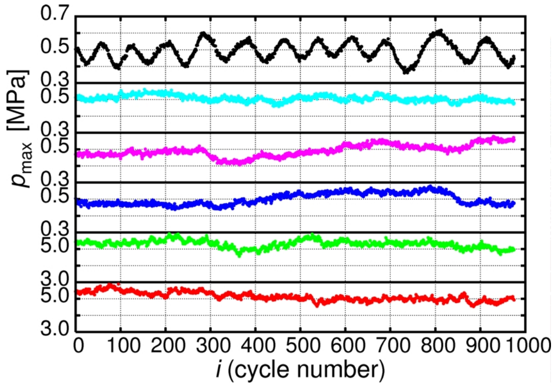


Fig. 2. Time series of cyclic peak pressure values $p_{\max}(i)$ for six different speeds of the crankshaft: $\Omega = 1000$, 1200, 1400, 1600, 1800 and 2000 rpm (starting from the bottom).

for the other five speeds of the crankshaft considered here.

## 3. Analysis of the Peak Pressure Time Series

Analyzing Fig. 2 one can see that in case of $\Omega = 2000$ strongly periodic components of the signal are observable while for other speeds $\Omega = 1000$, 1200, 1400, 1600, 1800 one cannot see any noticeable periodics. For better clarity we have performed RP and RQA. It should be noted that originally the RP method was invented to present signal data as patterns on a two-dimensional (time versus time) figure [27, 28]. After supplementing by the method of results quantification (RQA) it became an alternative to standard frequency analysis [29 – 33].

### *3.1. Recurrence Plots and Recurrence Quantification Analysis*

We now use the methods of RPs and RQA to examine the peak pressure time series for each of the six crankshaft speeds of $\Omega = 1000$, 1200, 1400, 1600, 1800 and 2000 rpm. For this purpose we embed each time series in a high-dimensional space using time-delay coordinates. Following Takens [34] we write

$$\mathbf{p}_{\max}(i) = [p_{\max}(i), p_{\max}(i-\delta i), p_{\max}(i-2\delta i), \ldots, p_{\max}(i-(m-1)\delta i)], \tag{1}$$

where $m$ is the embedding dimension and $\delta i$ is the time delay. For each time series we estimate the values of $m$ and $\delta i$ by calculating the average mutual information and the fraction of false nearest neighbours [35 – 38].

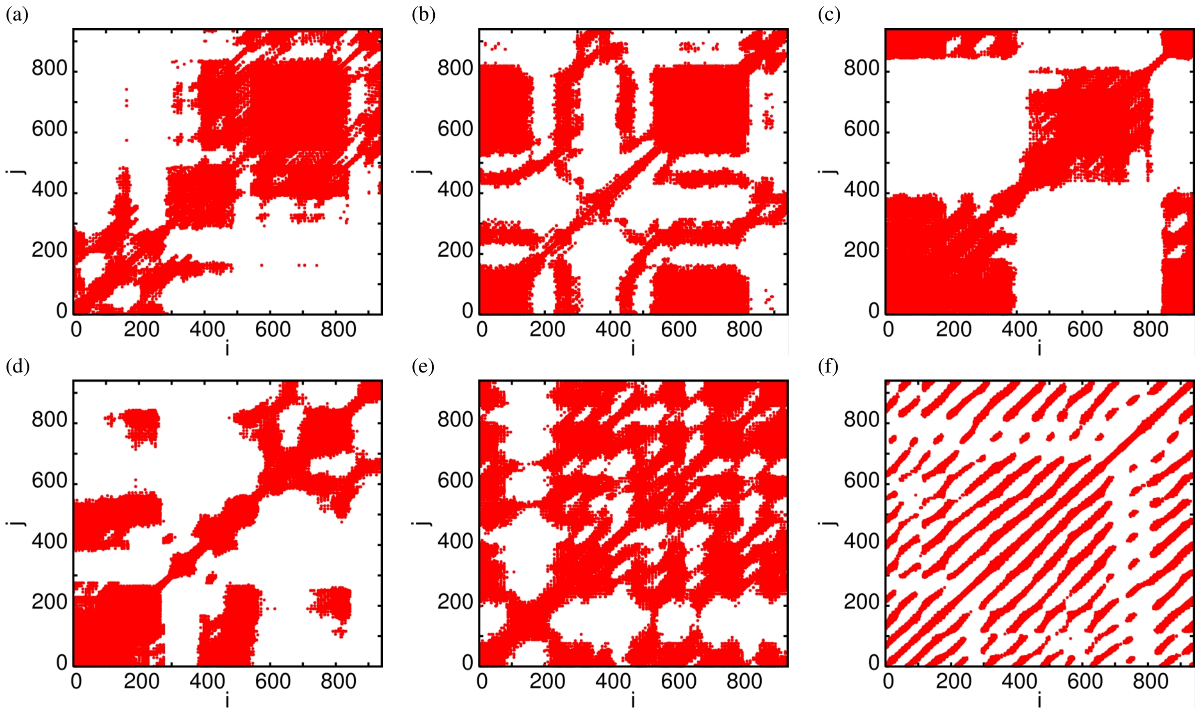


Fig. 3. Recurrence plots of the peak pressure time series for various speeds $\Omega$ of the crankshaft: (a) 1000 rpm; (b) 1200 rpm; (c) 1400 rpm; (d) 1600 rpm; (e) 1800 rpm; (f) 2000 rpm. The embedding dimension $m = 5$, delay $\delta i = 10$ and a Theiler window $w = 1$ have been used. For all cases the recurrence rate $RR$ is 0.15.

For subsequent analysis we use the smallest value of $\delta i$, $\delta i = 10$, and the largest value of $m$, $m = 5$, for all the time series.

The RP is constructed from the matrix $\mathbf{R}^{m,\varepsilon}$ with its elements $R_{ij}^{m,\varepsilon}$ given by [12, 33, 27 – 33]

$$R_{ij}^{m,\varepsilon} = \Theta(\varepsilon - \|\mathbf{p}_{\max}(i) - \mathbf{p}_{\max}(j)\|). \tag{2}$$

The elements 0 and 1 are translated into the RP as an empty space and a black dot, respectively, and $\varepsilon$ is a threshold value. By examining the patterns of diagonal, vertical and horizontal lines in an RP one can classify the dynamics of the system in a more quantitative fashion [31].

This is done by defining several parameters as described below.

The recurrence rate $RR$ is defined as

$$RR = \frac{1}{N^2} \sum_{i,j=1}^{N} R_{ij}^{m,\varepsilon}, \quad \text{for} \quad |i - j| \geq w. \tag{3}$$

This quantity determines the fraction of black dots in an RP. Here $w$ denotes the Theiler window used to exclude identical and neighbouring points from the above summation.

Using the distributions $P(l)$ and $P(v)$ of the lengths of diagonal and vertical lines, respectively, we now define parameters such as determinism ($DET$), laminarity ($LAM$) and trapping time ($TT$):

$$\begin{aligned} DET &= \sum_{l=l_{\min}}^{N} lP(l) \Big/ \sum_{l=1}^{N} lP(l), \\ LAM &= \sum_{v=v_{\min}}^{N} vP(v) \Big/ \sum_{v=1}^{N} vP(v), \\ TT &= \sum_{v=v_{\min}}^{N} vP(v) \Big/ \sum_{v=v_{\min}}^{N} P(v). \end{aligned} \tag{4}$$

In the above formulae $l_{\min} = v_{\min} = 2$ are the minimal length lines to be taken into account in the statistical analysis; see [31] for details.

These parameters describe various aspects of an RP and thus provide information about the different types of behaviour of the time series under consideration. The parameter $DET$ is a measure of the proportion of recurrence points forming diagonal line segments and reveals the existence of deterministic structures in the time series. $LAM$ is a similar parameter as $DET$, but is based on vertical line segments; it represents the extent

Table 1. RQA results for the peak pressure time series for various speeds $\Omega$ of the crankshaft. In all cases the embedding dimension $m = 5$, delay $\delta i = 10$, and a Theiler window $w = 1$ have been used, and $RR = 0.15$.

| $\Omega$ | *DET* | *LAM* | *TT* |
|---|---|---|---|
| 1000 | 0.8010 | 0.8644 | 6.019 |
| 1200 | 0.7172 | 0.8055 | 4.914 |
| 1400 | 0.7569 | 0.8246 | 5.094 |
| 1600 | 0.8267 | 0.8773 | 7.225 |
| 1800 | 0.6116 | 0.7266 | 3.634 |
| 2000 | 0.9260 | 0.9558 | 12.41 |

of laminar phase or intermittency, and $TT$ describes how long the system remains in a laminar phase.

Figures 3a – f present the RPs for the six peak pressure time series shown in Figure 2. Note that Fig. 3f ($\Omega = 2000$ rpm) consists mainly of diagonal lines indicating periodic oscillations. The period is given by the distance between the lines and is approximately 90. Periodic behaviour is also observed in Fig. 3b ($\Omega = 1200$ rpm) and Fig. 3e ($\Omega = 1800$ rpm). On the other hand, there are extensive white regions on the upper-left and lower-right corners in Fig. 3a ($\Omega = 1000$ rpm), Fig. 3c ($\Omega = 1400$ rpm) and Fig. 3d ($\Omega = 1600$ rpm). These white regions indicate the presence of a trend or other nonstationarity in the time series [31]. Furthermore, Fig. 3c ($\Omega = 1400$ rpm) indicates modulations of much larger period, but to confirm such a conclusion one has to examine longer time series [39].

Next we discuss the results of RQA which are presented in Table 1. In all cases considered here we used the same fixed recurrence rate $RR = 0.15$. Let us first examine the case of $\Omega = 2000$ rpm. Note that the values of *DET* and *LAM*, in this case, are the largest among all the cases. These parameters affirm the deterministic nature of the periodic oscillations.

Interestingly the other periodic cases $\Omega = 1200$ rpm and $\Omega = 1800$ rpm are characterized by smaller values of *DET* and *LAM*, which indicate less regular dynamics. This could be also related to the effect of a curved structure [40]. Curved structures in RPs can appear if the amplitude and/or frequency are modulated.

### *3.2. Wavelet Analysis*

For comparison we have also examined the various peak pressure-time series using wavelet analysis. In particular, we have used a continuous wavelet transform (CWT) [19, 24, 41] and computed the wavelet power spectra (WPS); these are shown in Figs. 4a – f.

Several dynamical features can be discerned from these figures. For instance, Fig. 4f, which applies for $\Omega = 2000$ rpm, clearly shows the presence of periodic oscillations with an approximate period of 90. This is consistent with the results shown in the RP of Figure 3f. Furthermore, oscillations with larger periods are observed in Figs. 4b and 4e. Some modulations of the period appear in Fig. 4e, as seen earlier in the RP of Figure 3e. In addition to these periodic structures, the wavelet spectra reveal oscillations of much shorter periods that appear intermittently. The intermittency is also reflected in the RQA parameters. Note that in all the cases *LAM* is larger than *DET* which implies a robust vertical structure (Figs. 3a – f) and is closely related to the appearance of laminarity and intermittency [42].

## 4. Concluding Remarks

Using RPs and RQA we have analyzed the cycle-to-cycle variations of the peak pressure in a diesel engine for six rotational speeds of the crankshaft. Our results indicate that depending on the engine speed, the pressure variations in the cylinder exhibit different types of behaviour ranging from periodic oscillations to intermittent fluctuations. These results have been verified by performing a wavelet analysis of the pressure-time series.

The above methods can be used for effective engine monitoring and for developing efficient strategies of engine control [43]. In particular, the RQA parameters can be used to quantify the maximum pressure variations that are represented by relatively short time series.

On the other hand, the trapping time parameter $TT$ is strictly related to the existence of short laminar phases in pressure fluctuations. Such laminar phases can be detected by both RPs and wavelet analysis. The trapping time associated with intermittent fluctuations is important for engine diagnostics. The desired situation would be to control combustion fluctuations in the engine, but an efficient feedback control requires predictability of cycle-to-cycle dynamics, at least in a short time range. The trapping time provides important information about the time scale of an engine response and about an optimal time delay needed in a control procedure [43].

Comparing the $TT$ parameter in cases of $\Omega = 1800$ and 2000 rpm, we see that it reaches the maximum for $\Omega = 2000$ and minimum for $\Omega = 1800$. Thus $TT$ could be also used for estimation of the proper working conditions.

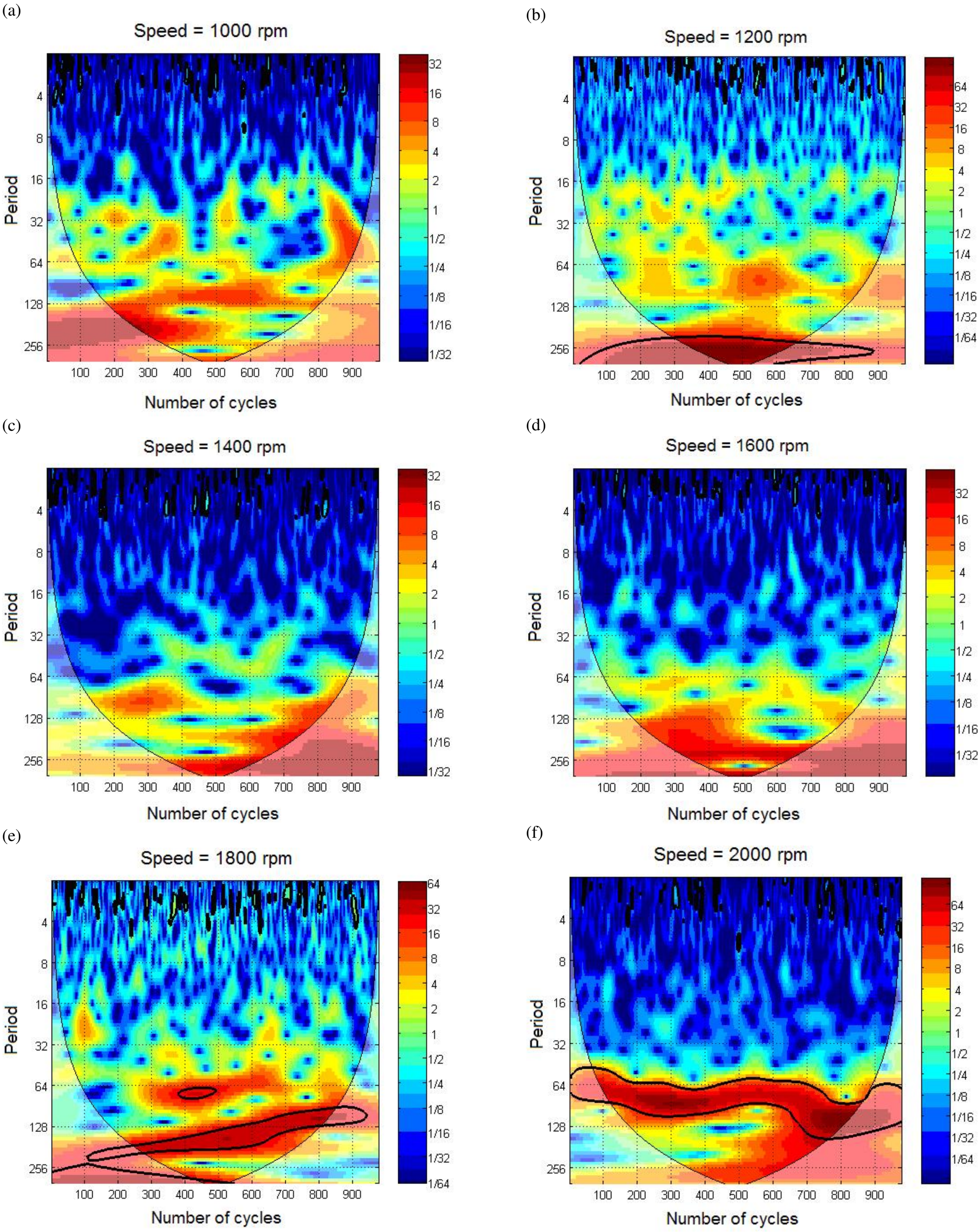


Fig. 4. Wavelet power spectra of the peak pressure-time series for various speeds $\Omega$ of the crankshaft: (a) 1000 rpm; (b) 1200 rpm; (c) 1400 rpm; (d) 1600 rpm; (e) 1800 rpm; (f) 2000 rpm. In these figures, the dark contours represent the 5% significance level, and the thin U-shaped curve denotes the cone of influence [39].

The large changes in $DET$, $LAM$ and $TT$ in two neighbouring cases, $\Omega = 1800$ and 2000 rpm (Table 1), could imply a bifurcation. The wavelet results (Figs. 4e and 4f denoted by contour lines) show that in the case of $\Omega = 1800$ rpm there are two important periods, 128 and 64, while for $\Omega = 2000$ rpm there is a single period of about 64 engine cycles. Note, that it is consistent with a period doubling bifurcation. Such a bifurcation could be also visible in Fig. 2 as the additional modulation and in the RP (Figs. 3e and 3f) as the smearing thickness of lines with an increasing distance between them.

*Acknowledgements*

The authors would like to thank Dr. K. Górski for his assistance in conducting the experiments and Prof. J. P. Zbilut for valuable comments. This research has been partially supported by the Polish Ministry for Science and Higher Education. G. L. would like to thank the Max Planck Institute for the Physics of Complex Systems in Dresden, Germany for hospitality.

[1] J. B. Heywood, Internal Combustion Engine Fundamentals, McGraw-Hill, New York 1988.
[2] R. E. Winsor and D. J. Patterson, Mixture turbulence, a key to cyclic combustion variation, SAE Paper No. 730086 (1973).
[3] J. C. Kantor, Science **224**, 1233 (1984).
[4] J. W. Daily, Combust. Sci. Technol. **57**, 149 (1988).
[5] A. P. Foakes and D. G. Pollard, Combust. Sci. Technol. **90**, 287 (1993).
[6] L. Chew, R. Hoekstra, J. F. Nayfeh, and J. Navedo, Chaos analysis of in-cylinder pressure measurements, SAE Paper No. 942486 (1994).
[7] Z. Hu, Nonlinear instabilities of combustion processes and cycle-to-cycle variations in spark-ignition engines, SAE Paper No. 961197 (1996).
[8] C. Letellier, S. Meunier-Guttin-Cluzel, G. Gouesbet, F. Neveu, T. Duverger, and B. Cousyn, Use of the nonlinear dynamical system theory to study cycle-to-cycle variations from spark-ignition engine pressure data, SAE Paper No. 971640 (1997).
[9] R. M. Wagner, J. A. Drallmeier, and C. S. Daw, Prior-cycle effects in lean spark ignition combustion-fuel/air charge considerations, SAE Paper No. 981047 (1998).
[10] R. M. Wagner, J. A. Drallmeier, and C. S. Daw, Int. J. Eng. Res. **1**, 301 (2001).
[11] M. Wendeker, J. Czarnigowski, G. Litak, and K. Szabelski, Chaos, Solitons, and Fractals **18**, 803 (2003).
[12] M. Wendeker, G. Litak, J. Czarnigowski, and K. Szabelski, Int. J. Bifurcat. Chaos **14**, 1801 (2004).
[13] C. S. Daw, C. E. A. Finney, J. B. Green Jr., M. B. Kennel, J. F. Thomas, and F. T. Connelly, A simple model for cyclic variations in a spark ignition engine, SAE Paper No. 962086 (1996).
[14] C. S. Daw, C. E. A. Finney, M. B. Kennel, and F. T. Connelly, Phys. Rev. E **57**, 2811 (1998).
[15] D. Scholl and S. Russ, Air-fuel ratio dependence of random and deterministic cyclic variability in a spark-ignited engine, SAE Paper No. 1999-01-3513 (1999).
[16] S. Russ, G. Lavoie, and W. Dai, SI engine operation with retarded ignition: part 1 – cyclic variations, SAE Paper No. 1999-01-3506 (1999).
[17] G. Litak, M. Wendeker, M. Krupa, and J. Czarnigowski, J. Vibr. Control **11**, 371 (2005).
[18] P. Bogus and J. Merkisz, Mech. Syst. Signal Proc. **19**, 881 (2005).
[19] A. K. Sen, R. Longwic, G. Litak, and K. Górski, Mech. Syst. Signal Proc. **22**, 362 (2008).
[20] R. Chiriac and N. Apostolescu, Cyclic variability patterns in a spark ignition engine fueled with LPG, SAE Paper No. 2004-01-1920 (2004).
[21] G.-X. Li and B.-F. Yao, Appl. Thermal Eng. **28**, 611 (2008).
[22] J. B. Green Jr., C. S. Daw, J. S. Armfield, C. E. A. Finney, R. M. Wagner, and J. A. Drallmeier, Time irreversibility and comparison of cyclic-variability models, SAE Paper No. 1999-01-0221 (1999).
[23] G. Litak, T. Kamiński, J. Czarnigowski, D. Żukowski, and M. Wendeker, Meccanica **42**, 423 (2007).
[24] A. K. Sen, G. Litak, R. Taccani, and R. Radu, Chaos, Solitons and Fractals **38**, 886 (2008).
[25] C. Piccardi and S. Rinaldi, Int. J. Bifurcat. Chaos **13**, 1579 (2003).
[26] G. Litak, R. Taccani, R. Radu, K. Urbanowicz, J. A. Holyst, M. Wendeker, and A. Giadrossi, Chaos, Solitons and Fractals **23**, 1695 (2005).
[27] J.-P. Eckmann, S. O. Kamphorst, and D. Ruelle, Europhys. Lett. **5**, 973 (1987).
[28] M. C. Casdagli, Physica D **108**, 12 (1997).
[29] N. Marwan, Encounters with Neighbours: Current Development of Concepts Based on Recurrence Plots and their Applications, PhD Thesis, Universität Potsdam, Potsdam 2003.
[30] N. Marwan, Recurrence Plots Code, http://www.agnld.uni-potsdam.de/~marwan/6.download/rp.php (2006).

[31] N. Marwan, M. C. Romano, M. Thiel, and J. Kurths, Phys. Rep. **438**, 237 (2007).
[32] C. L. Webber Jr. and J. P. Zbilut, J. Appl. Physiol. **76**, 965 (1994).
[33] M. Thiel, M. C. Romano, P. L. Read, and J. Kurths, Chaos **14**, 234 (2004).
[34] F. Takens, in: Lecture Notes in Mathematics, 898 (Eds. D. A. Rand and L.-S. Young), Springer, Berlin 1981, p. 366.
[35] H. Kantz and T. Schreiber, Non-Linear Time Series Analysis, Cambridge University Press, Cambridge 1997.
[36] A. M. Fraser and H. L. Swinney, Phys. Rev. A **33**, 1134 (1986).
[37] M. B. Kennel, R. Brown, and H. D. I. Abarbanel, Phys. Rev. A **45**, 3403 (1992).
[38] R. Hegger, H. Kantz, and T. Schreiber, Chaos **9**, 413 (1999).
[39] T. Kaminski, M. Wendeker, K. Urbanowicz, and G. Litak, Chaos **14**, 461 (2004).
[40] A. Facchini and H. Kantz, Phys. Rev. E **75**, 036215 (2007).
[41] C. Torrence and G. P. Compo, Bull. Am. Meteorol. Soc. **79**, 61 (1988).
[42] N. Marwan, N. Wessel, U. Meyerfeldt, A. Schirdewan, and J. Kurths, Phys. Rev. E **66**, 026702 (2002).
[43] K. Matsumoto, I. Tsuda, and Y. Hosoi, Z. Naturforsch. **62a**, 587 (2007).